Monthly Notices
of the
ROYAL ASTRONOMICAL SOCIETY

MNRAS **475,** 2835–2841 (2018)
Advance Access publication 2018 January 5

doi:10.1093/mnras/stx3350

Hall effect in the coma of 67P/Churyumov–Gerasimenko

Z. Huang,[1]★ G. Tóth,[1] T. I. Gombosi,[1] X. Jia,[1] M. R. Combi,[1] K. C. Hansen,[1] N. Fougere,[1] Y. Shou,[1] V. Tenishev,[1] K. Altwegg[2] and M. Rubin[2]

[1]*Climate and Space Sciences and Engineering, University of Michigan, Ann Arbor, MI 48109, USA*
[2]*Physikalisches Institut, University of Bern, CH-3012 Bern, Switzerland*

Accepted 2017 December 23. Received 2017 November 21; in original form 2017 September 26

ABSTRACT

Magnetohydrodynamics simulations have been carried out in studying the solar wind and cometary plasma interactions for decades. Various plasma boundaries have been simulated and compared well with observations for comet 1P/Halley. The *Rosetta* mission, which studies comet 67P/Churyumov–Gerasimenko, challenges our understanding of the solar wind and comet interactions. The Rosetta Plasma Consortium observed regions of very weak magnetic field outside the predicted diamagnetic cavity. In this paper, we simulate the inner coma with the Hall magnetohydrodynamics equations and show that the Hall effect is important in the inner coma environment. The magnetic field topology becomes complex and magnetic reconnection occurs on the dayside when the Hall effect is taken into account. The magnetic reconnection on the dayside can generate weak magnetic field regions outside the global diamagnetic cavity, which may explain the Rosetta Plasma Consortium observations. We conclude that the substantial change in the inner coma environment is due to the fact that the ion inertial length (or gyro radius) is not much smaller than the size of the diamagnetic cavity.

Key words: MHD – comets: individual: Comet 67P/Churyumov–Gerasimenko – planet–star interactions.

1 INTRODUCTION

Cometary magnetosphere is one of the most important topics in planetary science. Because the nucleus of a comet is usually very small in size ranging from a few hundred metres to tens of kilometres (e.g. the radius of the nucleus for comet 1P/Halley is about 10 km) and the gravity is extremely weak (usually considered negligible when simulating the cometary neutral gas and plasma), the cometary coma is much larger in size compared to the nucleus itself. For example, *Giotto* observed plasma boundaries of comet 1P/Halley starting at roughly 1 Mkm away from the nucleus (Reme et al. 1986). The cometary magnetosphere resulting from the solar wind interaction with the coma has some distinct features from the magnetospheres associated with planets or planetary moons, such as the formation of a diamagnetic cavity. Gombosi (2015) provided an excellent review of the cometary magnetosphere. A typical cometary magnetosphere for an active comet near perihelion includes a bow shock that slows down the supersonic solar wind to subsonic speed (Galeev, Cravens & Gombosi 1985; Koenders et al. 2013), a diamagnetic cavity inside which the magnetic field drops to zero (Neubauer et al. 1986; Cravens 1986; Goetz et al. 2016a,b), a recombination layer that separates the inner shock (which slows down the supersonic cometary ion outflow to subsonic), and the contact surface (where the solar wind protons cannot penetrate). One of the primary goals of the Rosetta Plasma Consortium (RPC) was to observe the evolution of the solar wind and comet interactions. However, due to the close proximity of the *Rosetta* spacecraft to the nucleus, RPC was not able to observe the bow shock. Also the recombination layer and contact surface have not been clearly identified to date. Based on RPC observations, Mandt et al. (2016) reported plasma boundaries separating an inner region and an outer region, and they concluded the observed plasma boundaries are an ion-neutral collisionopause boundary, which has not been predicted by previous numerical simulations (Koenders et al. 2015; Rubin et al. 2015; Huang et al. 2016a). In addition to this unpredicted boundary, the magnetic field observed by RPC is also unexpected: the diamagnetic 'cavity' (Goetz et al. 2016a,b), was observed much farther away than the predicted locations (Koenders et al. 2015; Rubin et al. 2015; Huang et al. 2016a).

A Lot of effort has been made in numerical simulations to understand the solar wind and comet interactions. There are two major approaches in simulating the cometary environment: the fluid approach (Gombosi et al. 1996; Hansen et al. 2007; Rubin et al. 2014, 2015; Huang et al. 2016a) and the hybrid approach (Bagdonat & Motschmann 2002; Koenders et al. 2015; Wedlund et al. 2017). In a fluid approach, the plasma is treated as fluids and governed by the magnetohydrodynamic (MHD) equations. The fluid approach is an accurate description of the macroscopic quantities of the plasma when the Knudsen number ($K_n = \frac{\lambda}{l}$, where λ is the mean free path

★ E-mail: zghuang@umich.edu

and l is the characteristic length-scale of the flow) is much smaller than unity. On the other hand, the hybrid approach simulates ions as individual particles and electrons as a fluid. The hybrid approach can capture the kinetic features of the plasma and works well also for large Knudsen numbers. Compared to the fluid approach, the hybrid approach is very computationally expensive and is usually limited to a small simulation domain. Recently, a third approach to simulate the solar wind and comet interactions was developed by Deca et al. (2017) with a fully kinetic code, which treats both ions and electrons as particles. They simulated comet CG at 3 au and showed that their simulations agreed well with RPC observations at that heliocentric distance. However, their code does not include any chemical reactions and collisions between particles, which makes it not applicable to comets near perihelion, where chemical reactions are important. Also their model is limited to a small domain that does not include the bow shock.

There have been extensive discussions about whether fluid codes can properly simulate cometary environments or those of other planets/moons without an intrinsic magnetic field, in which case the ion gyro radius is larger than the length-scale of interaction regions. We argue that fluid codes are not limited exclusively by the requirement that the length-scale must be much larger than the ion gyro radius, because collisions among different particles as well as chemical reactions may reduce the ion kinetic effects arising from the gyro motion. It is true that single fluid ideal MHD models cannot capture any ion gyration effects compared to a hybrid simulation (Hansen et al. 2007). But when fluid simulations take into account different fluids with different velocities as well as collisions among them, multifluid MHD models are capable of capturing some important ion kinetic behaviours. For example, Rubin et al. (2014) showed that their multifluid MHD model is capable of resolving the gyration of different ion fluids with reasonably good agreement with what has been predicted by a hybrid model (Müller et al. 2011). The major discrepancy lies in the very inner coma region with striations/filaments in the cometary ion density (Koenders et al. 2015). On the other hand, multifluid simulations for other planets/moons without an intrinsic magnetic field have demonstrated that the simulation results agree well with in situ plasma observations (Ma et al. 2011; Najib et al. 2011; Bougher et al. 2015). Hybrid models certainly provide a better description of the plasma environment near the comet nucleus. However, it is much more expensive or nearly impossible to computationally run hybrid models with a grid resolution comparable to those of fluid models on a large enough domain to properly set up the outer boundary conditions and to resolve the details of a diamagnetic cavity formed close to the nucleus. With a relatively coarse grid typically used in hybrid models, effects of numerical diffusion are expected to be much stronger than in fluid models, and in such a case, the evolution of the magnetic field may not be properly described. As described below, the multifluid Hall MHD model presented in this paper represents another step in further resolving kinetic effects with fluid simulations.

One of the imperfections of previous MHD models applied in cometary studies is that the Hall effect is usually not taken into account. The Hall effect describes the relative speed (current) between ions and electrons and appears in the generalized Ohm's law. This current may affect the magnetic field evolution in the system if the Hall effect is taken into account in the induction equation. The Hall effect is important in magnetic reconnection studies as Hall MHD is the minimal modification of resistive MHD that can reproduce the fast reconnection process (Birn et al. 2001), partially due to the strong current near the reconnection null point. In the cometary magnetosphere, the diamagnetic cavity is a unique feature that other planets/moons do not have. As the magnetic field drops to zero in a short distance, there must be strong currents along the diamagnetic cavity boundary. How these currents affect the inner coma environment is still unknown. In this paper, we simulate the inner coma environment with Hall MHD equations and show that the Hall effect is important in the inner coma and the classical plasma boundaries obtained by previous models need to be revisited.

2 THE HALL MHD MODEL

Our Hall MHD model is an extension of the multifluid model developed by Huang et al. (2016a). In the following equations, mass density, velocity vector, pressure, the identity matrix, and the adiabatic index are denoted by symbols ρ, $\boldsymbol{u}$, p, $\mathbf{I}$, and γ, respectively. The cometary neutral gas, the ions (cometary and solar wind), and the electrons are denoted by subscripts n, s, and e, respectively. The symbol Z denotes the ion charge state, whereas the symbol e is for the unit charge.

There are four fluids in the model. One fluid describes the cometary neutral gas with the Euler equations:

$$\frac{\partial \rho_{\rm n}}{\partial t} + \nabla \cdot (\rho_{\rm n} \boldsymbol{u}_{\rm n}) = \frac{\delta \rho_{\rm n}}{\delta t}, \tag{1a}$$

$$\frac{\partial \rho_{\rm n} \boldsymbol{u}_{\rm n}}{\partial t} + \nabla \cdot (\rho_{\rm n} \boldsymbol{u}_{\rm n} \boldsymbol{u}_{\rm n} + p_{\rm n} \mathbf{I}) = \frac{\delta \rho_{\rm n} \boldsymbol{u}_{\rm n}}{\delta t}, \tag{1b}$$

$$\frac{\partial p_{\rm n}}{\partial t} + \nabla \cdot (p_{\rm n} \boldsymbol{u}_{\rm n}) + (\gamma_n - 1) p_{\rm n} (\nabla \cdot \boldsymbol{u}_{\rm n}) = \frac{\delta p_{\rm n}}{\delta t}, \tag{1c}$$

and the other two fluids describe the cometary ions and the solar wind protons with the multifluid MHD equations, which are solved individually for both fluids:

$$\frac{\partial \rho_s}{\partial t} + \nabla \cdot (\rho_s \boldsymbol{u}_s) = \frac{\delta \rho_s}{\delta t}, \tag{2a}$$

$$\frac{\partial \rho_s \boldsymbol{u}_s}{\partial t} + \nabla \cdot (\rho_s \boldsymbol{u}_s \boldsymbol{u}_s + p_s \mathrm{I}), \\ - Z_s e \frac{\rho_s}{m_s} (\boldsymbol{E} + \boldsymbol{u}_s \times \boldsymbol{B}) = \frac{\delta \rho_s \boldsymbol{u}_s}{\delta t}, \tag{2b}$$

$$\frac{\partial p_s}{\partial t} + \nabla \cdot (p_s \boldsymbol{u}_s) + (\gamma_s - 1) p_s (\nabla \cdot \boldsymbol{u}_s) = \frac{\delta p_s}{\delta t}. \tag{2c}$$

For the electrons, we do not specify the continuity and momentum equations. Assuming charge neutrality in the plasma, the electron number density can be obtained as $n_{\rm e} = \sum_{s=\rm ions} Z_s n_s$. The electron velocity $\boldsymbol{u}_e$ is obtained from $\boldsymbol{u}_{\rm e} = \boldsymbol{u}_+ + \boldsymbol{u}_{\rm H}$, where $\boldsymbol{u}_+$ is the charge averaged ion velocity ($\boldsymbol{u}_+ = \frac{\sum_{s=\rm ions} Z_s n_s \boldsymbol{u}_s}{n_{\rm e}}$) and $\boldsymbol{u}_{\rm H}$ is the Hall velocity ($\boldsymbol{u}_{\rm H} = -\frac{\boldsymbol{j}}{n_{\rm e} e}$, where $\boldsymbol{j}$ is the current density $\boldsymbol{j} = (1/\mu_0) \nabla \times \boldsymbol{B}$). The electron pressure in the system is described by

$$\frac{\partial p_{\rm e}}{\partial t} + \nabla \cdot (p_{\rm e} \boldsymbol{u}_{\rm e}) + (\gamma_{\rm e} - 1) p_{\rm e} (\nabla \cdot \boldsymbol{u}_{\rm e}) = \frac{\delta p_{\rm e}}{\delta t}. \tag{3}$$

We use equations (1)–(3) to describe the behaviour and interactions of different fluids (the cometary neutral gas, the cometary ions, the solar wind protons, and the electrons) in the system. Ionization (photoionization and electron impact ionization) of the cometary neutral gas, charge exchange between neutrals and ions, collisions (elastic and inelastic) between different fluids, and recombination are all taken into account in simulating the cometary environment

and they appear as source terms in the right-hand side of equations (1)–(3). We apply the same source terms as Huang et al. (2016a). The stiffness of the source terms may limit the time step, so a point-implicit algorithm (Tóth et al. 2012) is applied to evaluate these terms.

The electric and magnetic fields are also needed to solve the multifluid equations. The electric field is derived from the electron momentum equation if the inertial terms are assumed to be zero (due to the small electron mass):

$$\boldsymbol{E} = -\boldsymbol{u}_{\rm e} \times \boldsymbol{B} - \frac{1}{n_{\rm e} e} \nabla p_{\rm e}. \quad (4)$$

The magnetic field is obtained from the induction equation:

$$\frac{\partial \boldsymbol{B}}{\partial t} = -\nabla \times \boldsymbol{E}. \quad (5)$$

We solve equations (1)–(5) on a 3D block adaptive grid with the BATS-R-US (Block-Adaptive Tree Solarwind Roe-type Upwind Scheme) code (Powell et al. 1999; Tóth et al. 2012). The beauty of the adaptive grid is that we can resolve different length-scales in the system, so that the simulation can resolve the nucleus while modelling the global scales. In the comet CG case, the radius of the nucleus is about 2 km, the global diamagnetic cavity is reported to be about 100 km, and the bow shock is expected to be at about 8000 km upstream of the nucleus (Koenders et al. 2015; Rubin et al. 2015; Huang et al. 2016a). In our simulation, the smallest cell is located near the nucleus with the size of about 0.12 km and the largest cell is located near the outer boundary with the size of about 31 250 km, which requires 18 levels of refinements (each refinement level increases the resolution by a factor of 2) in the domain. We use the cometocentric solar equatorial (CSEQ) frame in the simulation. In this frame, +x points towards the Sun, the z axis contains the solar rotation axis, and the y axis is orthogonal to the x and z axes. The solar wind is considered to move along the $-x$ direction with the interplanetary magnetic field points in the $+y$ direction at the upstream boundary. The simulation box is within $\pm 10^6$ km in the x direction and $\pm 0.5 \times 10^6$ km in both y and z directions. We specify boundary conditions the same way as Huang et al. (2016a) at the edge of the simulation box (outer boundary) as well as at the nucleus surface (inner boundary).

In this study, the cometary neutral gas is limited to water molecules with the specific heat ratio (γ) of 4/3 and the corresponding cometary ions are H_2O^+ with the same γ. $\gamma = 5/3$ applied for the solar wind protons as well as electrons. An idealized spherical comet with the neutral gas outflow driven by the solar illumination (hereafter illuminated sphere) seems to be the minimum requirement not to lose important asymmetrical features in the inner coma (Huang et al. 2016a), so we apply this nucleus condition at the inner boundary, which is the same as Case 2 in Huang et al. (2016a). We apply the same input parameters listed in tables 2 and 3 in Huang et al. (2016a). We first run the multifluid model in steady-state mode without the Hall effect to reach a steady state. We then introduce the Hall effect at $t = 0$ and run the model in time-dependent mode to investigate the evolution of the inner coma.

3 SIMULATION RESULTS

Fig. 1 shows the multifluid Hall MHD simulation results in the inner coma region (within 400 km of the nucleus) with an illuminated sphere at $t = 600$ s. Although the simulation results preserve symmetries about the y axis in the $z = 0$ plane, they show pronounced asymmetries in the $y = 0$ plane. As a comparison, we reproduce the multifluid simulation results without the Hall effect in the same region with an illuminated sphere for the same input parameters (Case 2 in Huang et al. 2016a) in Fig. 2. In Huang et al. (2016a), the size of the diamagnetic cavity and the location of the contact surface agreed well with previous MHD simulations (Rubin et al. 2015) and hybrid simulations (Koenders et al. 2015). However, when the Hall effect is introduced, the ion pile-up region (with light yellow colour) in the upper panel is distorted in the $y = 0$ plane and looks completely different from the upper panel of Fig. 2, where the distribution is symmetric about the z axis. Some surface wave structures, which might be associated with the Kelvin–Helmoltz (hereafter K–H) instabilities reported in Rubin et al. (2012), can also be found in the upper panel of Fig. 1.

The magnetic field topology in the bottom panels of Fig. 1 is completely different from the bottom panels of Fig. 2. When the model does not include the Hall effect, the diamagnetic cavity (bottom panels of Fig. 2) is an isolated region and the magnetic field pile-up region is just upstream of the diamagnetic cavity. When the Hall effect is introduced, the magnetic field configuration becomes more complex and besides the 'global' diamagnetic cavity, regions of very weak magnetic field (less than 10 nT) can also be found in the lower right-hand corner in the $y = 0$ plane in the bottom left-hand panel of Fig. 1. We suggest that it is the $\boldsymbol{J} \times \boldsymbol{B}$ force discussed in the next paragraph that changes the magnetic field configuration in the inner coma region. The magnetic field pile-up region in the $y = 0$ plane is shifted and is not located in the same region as in Fig. 2. In the $z = 0$ plane (the bottom right-hand panels of both Figs 1 and 2), the diamagnetic cavity looks more or less the same between the two simulations. The biggest difference lies in the magnetic pile-up region. In Fig. 1, only two small magnetic field pile-up regions are found outside the diamagnetic cavity, whereas in Fig. 2, the magnetic pile-up region is a single region.

It is quite surprising that the simulated magnetic field changes so dramatically when the Hall effect is taken into account in the induction equation. Besides, the Hall MHD simulation does not have a steady-state solution despite the fixed upstream solar wind conditions. The online movie ('inner_coma_movie.mp4') shows the evolution of the cometary ion density (with velocity streamlines) and the magnetic field between $t = 421$ and 600 s. In the movie, the cometary ions move in the negative z direction. To illustrate this, we plot a snapshot of the cometary ion density with velocity streamlines at $t = 600$ s in the upper panel of Fig. 3. This motion of the cometary ions can be explained by the $\boldsymbol{J} \times \boldsymbol{B}$ force, which is plotted in the bottom panel of Fig. 3. This figure shows that along the global diamagnetic cavity boundary, the $\boldsymbol{J} \times \boldsymbol{B}$ force has a negative z component, which acts to move the cometary ions in the negative z direction.

Another important new observation from the Hall MHD simulation is the formation of the weak magnetic field regions in the lower right-hand corner of Fig. 1. These structures appear as quasi-periodic structures in the online movie ('inner_coma_movie.mp4'). We provide a best estimate of the periods ranging from 10 to 50 s, which are a combination of different harmonic periods, based on the evolution of the magnetic pile-up regions in the online movie ('inner_coma_movie.mp4'). The periods depend on many factors, e.g. the plasma flow speed compared to the Alfvén speed, the strength of the currents as well as the direction and magnitude of the $\boldsymbol{J} \times \boldsymbol{B}$ force. It is impossible to calculate the exact periods in such a complex case. To investigate how these weak magnetic field regions form, we have examined the evolution of the magnetic field topology in 3D, which is animated in another two online movies (with

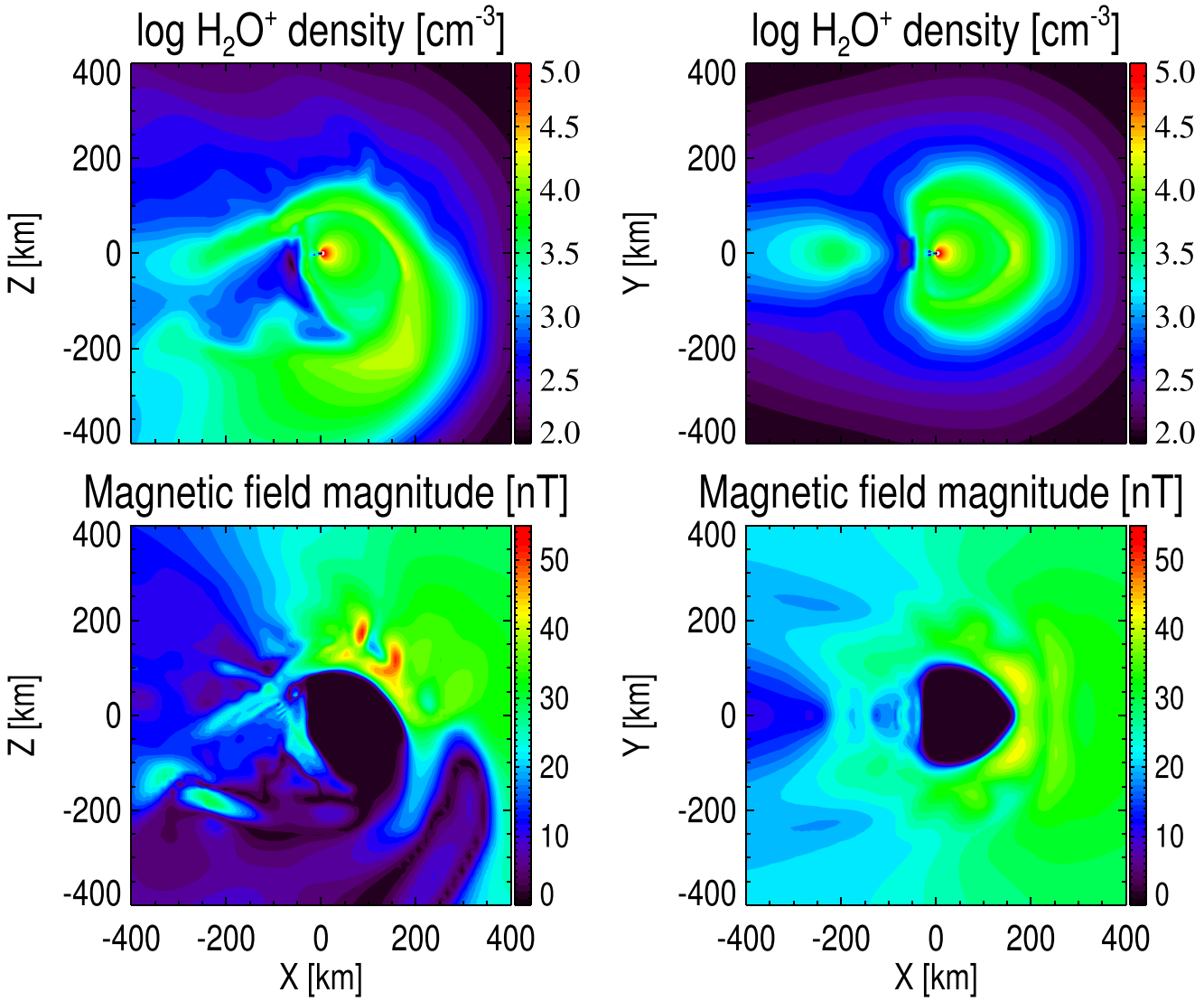

Figure 1. The Hall MHD simulation results. The left-hand columns plot the $y = 0$ plane, whereas the right-hand columns plot the $z = 0$ plane. The upper panels are for the cometary ion density, whereas the lower panels show the magnetic field magnitude.

different view angles, 'reconnection_movie_view1.avi' and 'reconnection_moive_view2.avi'). In the plasma, the magnetic field is approximately frozen into the electron fluid. Both the cometary ions in the coma and the electrons move in the negative z direction (with the velocities separated by the currents). As the magnetic field moves with the electrons, the magnetic field is then draped in the negative z direction. A recent hybrid simulation by Koenders et al. (2016) also showed the draping signatures for comet CG at 2.0 au. In the Hall MHD simulation, the draping of the magnetic field lines forms a configuration that favours magnetic reconnections. The online movies only animate 15 s of the evolution (between $t = 425$ and 440 s), but they clearly show how the magnetic field reconnects and forms magnetic flux ropes. The magnetic reconnection reduces the magnetic field magnitude and create the weak magnetic field regions. Fig. 4 plots the 3D magnetic field configuration. Magnetic reconnections are expected to occur where the magnetic field lines bend strongly, denoted by an 'X' mark on the figure. As magnetic reconnections occur, outflow is expected at the magnetic null point with opposite directions. Fig. 5 confirms that the plasma moves oppositely on the two sides. The outflow speed is close to the Alfvén speed near the reconnection regions, which is in the order of 1 km s^{-1}.

Why does the Hall effect matter in the inner coma of comet CG? We argue that it is because the scale of the diamagnetic cavity is comparable to the ion inertial length ($d_{\rm i} = \frac{m_{\rm i}}{q_{\rm i}}\sqrt{\frac{1}{\rho_{\rm i}\mu_0}}$, where $m_{\rm i}$ is the ion mass, $q_{\rm i}$ is the ion charge, $\rho_{\rm i}$ is the ion mass density, and μ_0 is the magnetic permeability of vacuum) and the ion gyro radius ($r_i = \frac{v_{\rm th,i} m_{\rm i}}{q_{\rm i} B}$, where $v_{\rm th,\,i}$ is the ion thermal speed, and B is the magnetic field magnitutde). In the inner coma, the cometary ions dominate, so the ion inertial length and the gyro radius for the cometary ions are responsible for the physical processes. Fig. 6 plots the ion inertial length and the gyro radius for the cometary ions. The ion inertial length is slightly less than 10 km in the ion pile-up region, and it is in the order of 100 km outside the global diamagnetic cavity and the ion pile-up region. The gyro radius is very large where the magnetic field is small. Except in the weak magnetic field regions, the gyro radius has similar distributions as the ion inertial length. As the size of the global diamagnetic cavity is about 100 km, the ion inertial length and the ion gyro radius are

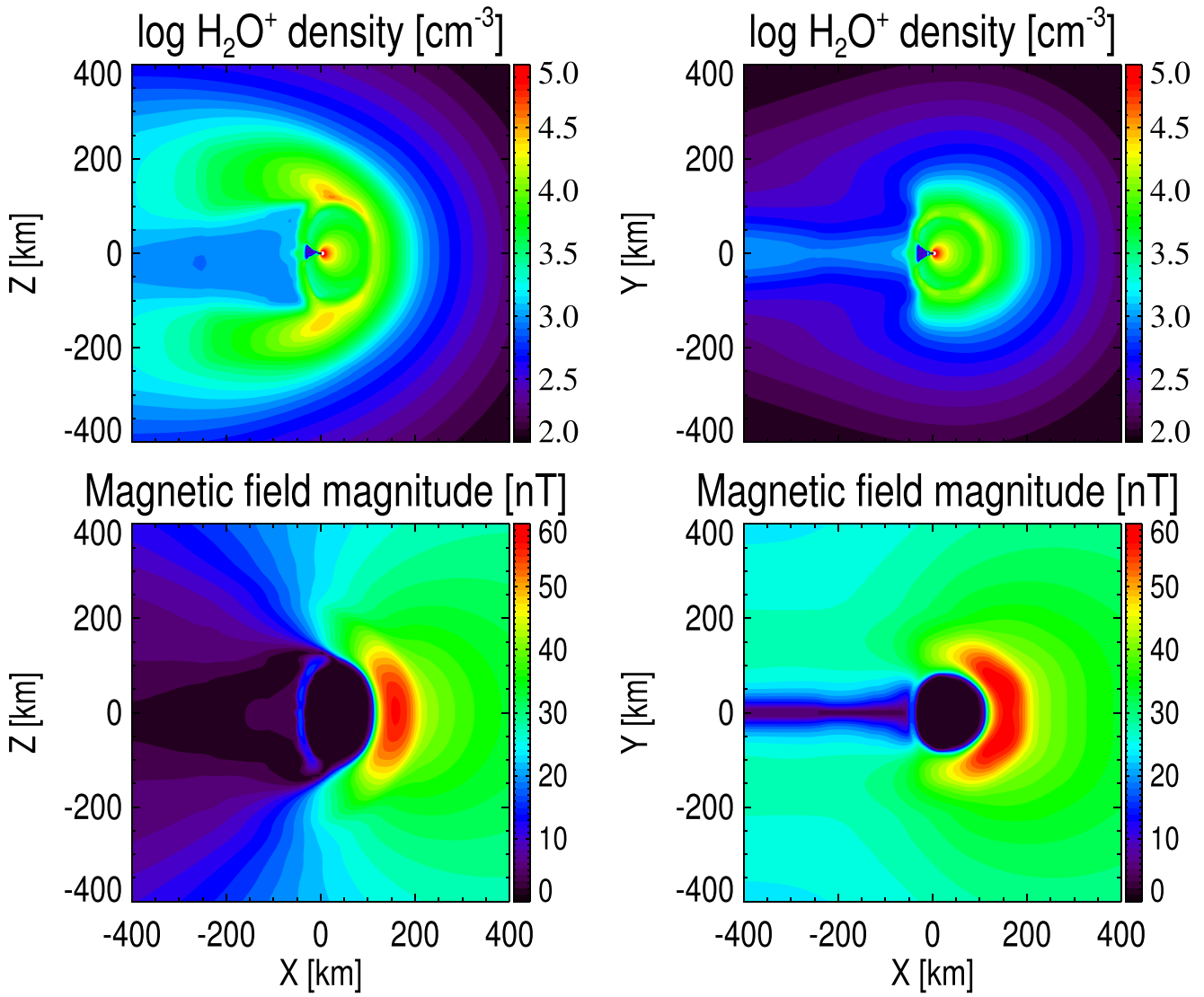

Figure 2. A reproduction of the simulation results from Huang et al. (2016a). Multifluid MHD results without the Hall effect to be compared with Fig. 1.

not much smaller than the global diamagnetic cavity. Dorelli et al. (2015) showed that Hall currents within the magnetopause and magnetotail current sheets have a significant impact on the global structure of Ganymede's magnetosphere because the magnetopause standoff distance is not much larger (order of 10) than the ion inertial length. In our case, the ratio of the size of the diamagnetic cavity and the ion inertial length (or gyro radius) is in order of 10 or less. We put forward an argument that if the ion inertial length (or gyro radius) is not much smaller than the characteristic length of the magnetosphere (the diamagnetic cavity in our case, the magnetopause standoff distance in Ganymede's magnetosphere), Hall MHD simulations are necessary to capture the correct global structure of the magnetosphere.

4 SUMMARY AND DISCUSSIONS

In this work, we performed a multifluid Hall MHD simulation to study the cometary plasma environment in the inner coma region of comet 67P/Churyumov–Gerasimenko. With the same model set up as Huang et al. (2016a), the Hall MHD simulation shows a very different picture: The inner coma is no longer symmetric and low magnetic field regions can form outside the global diamagnetic cavity and the solution is time-dependent.

The only difference between the Hall MHD simulation and the classical MHD simulations by Huang et al. (2016a) is that the Hall velocity term is considered in the magnetic induction equation, which means that the current can affect the evolution of the magnetic field. It is well known that the Hall effect is important in magnetic reconnections (Birn et al. 2001), partially due to relative weak magnetic field and strong currents near the magnetic null point. Hall MHD simulations of the magnetospheres of planets and moons typically do not show significant differences compared to the classical MHD simulations except in the regions where magnetic reconnections occur like the dayside magnetopause or the nightside magnetotail. Dorelli et al. (2015) reported that Hall effect is important in Ganymede's magnetosphere because the magnetopause standoff distance is in the order of 10 times larger than the ion inertial length. One would not expect the Hall MHD simulations dramatically to change the simulated inner coma environment for a comet because magnetic field reconnections have

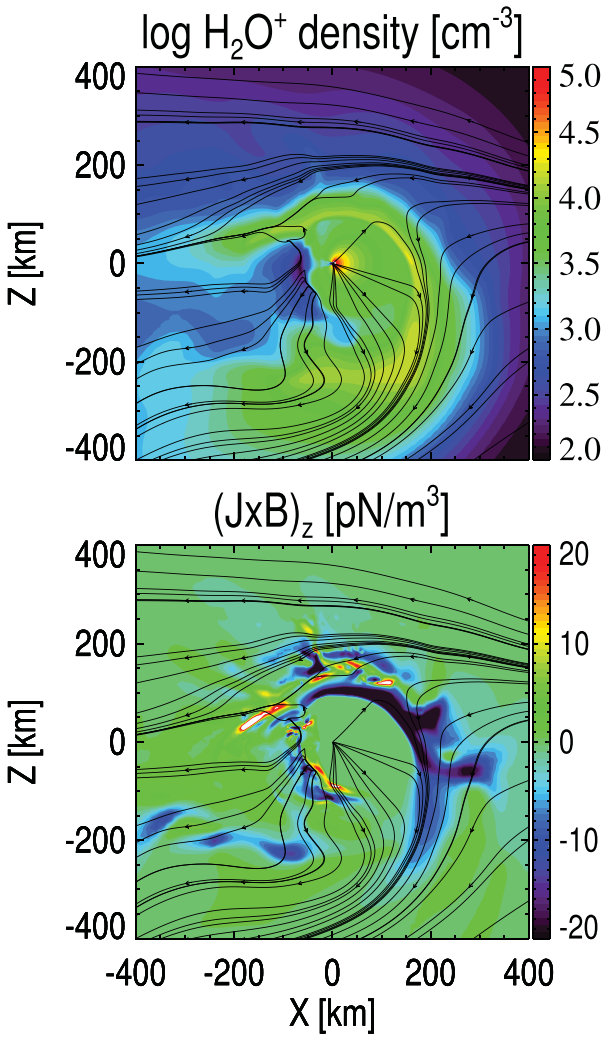

Figure 3. The upper panel shows the cometary ion density with their streamlines on the $y = 0$ plane. The bottom panel plots the z component of the $\boldsymbol{J} \times \boldsymbol{B}$ force density (in the unite of 1×10^{-12} N m^{-3}) on the $y = 0$ plane.

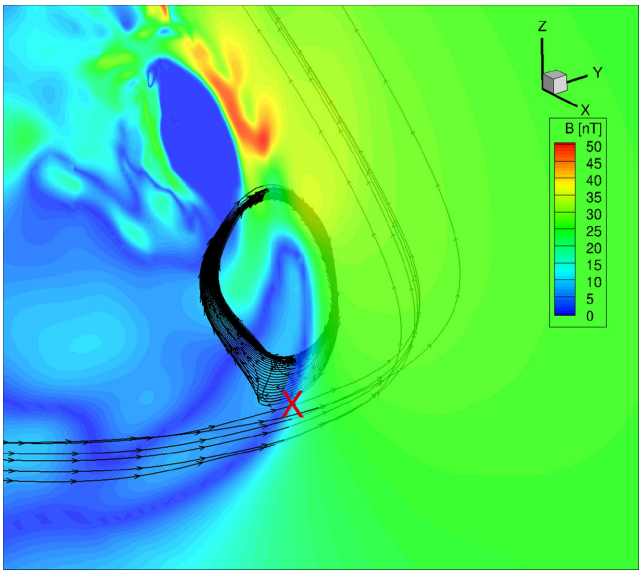

Figure 4. A 3D view of the magnetic field lines. The contour shows the magnetic field magnitude at the $y = 0$ plane. Magnetic reconnection is expected to occur near the red cross mark.

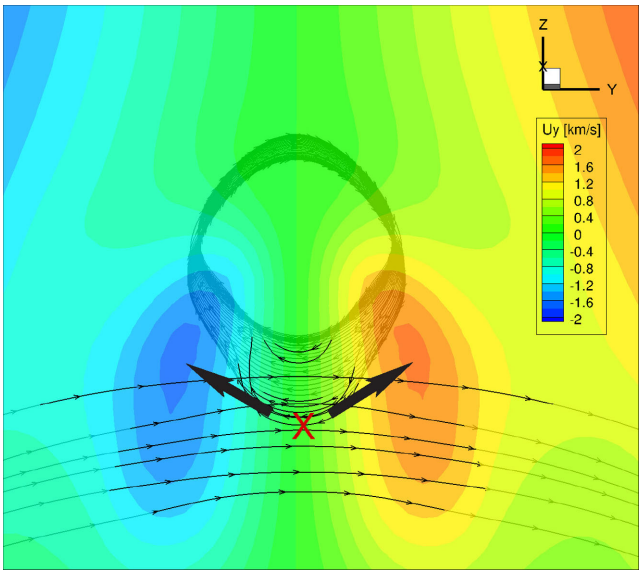

Figure 5. The U_y component for the cometary ion velocity at the surface close to the magnetic reconnection surface, which is defined by three points: [480, 0, 0], [500, 20, 33.5], and [460, 0, −33.5] km. The cometary ions move to the $+y$ direction on the right-hand side, whereas they move to the $-y$ direction on the left-hand side, near the magnetic null point denoted by the red cross mark, as indicated by the two black arrows.

only been reported on the nightside (Huang et al. 2016a), but our simulations show that in fact the results change dramatically.

The diamagnetic cavity is a unique feature in the cometary environment, which is not shared by other planets or moons in the Solar system, and it has received lots of attention since the *Giotto* mission (Cravens 1986; Neubauer et al. 1986; Goetz et al. 2016a,b; Huang et al. 2016b; Madanian et al. 2017). However, it has not been realized that currents along the diamagnetic cavity boundary may change the global structure of the inner coma. In the comet CG case, as the ion inertial length (or gyro radius) is not much smaller than the size of the global diamagnetic cavity, the Hall effect plays an important role in the evolution of the cometary plasma environment in the inner coma region, which is confirmed by our Hall MHD simulation. The situation might be different for a much more active comet. For example, the size of the diamagnetic cavity for comet 1P/Halley is about 4500 km (Neubauer et al. 1986; Cravens 1986), which will need to be compared with the ion inertial length (or gyro radius) to see whether the Hall effect is important there.

The most important feature from the Hall MHD simulations is that there can be dayside magnetic reconnection, which can create weak magnetic field regions outside the global diamagnetic cavity. One of the most puzzling observations from the RPC is that the magnetometer observed weak magnetic field at a distance much farther away than the predicted diamagnetic cavity. Goetz et al. (2016b, 2016a) explained the weak magnetic field observations as K–H instabilities propagating along the cavity boundary and Huang et al. (2016b) explained them as short-lived enhanced electron pressure along magnetic field lines. The Hall MHD simulation may provide a third option, magnetic field reconnection on the dayside. Further investigation and data comparison is necessary, but at this point, we refer this to future studies.

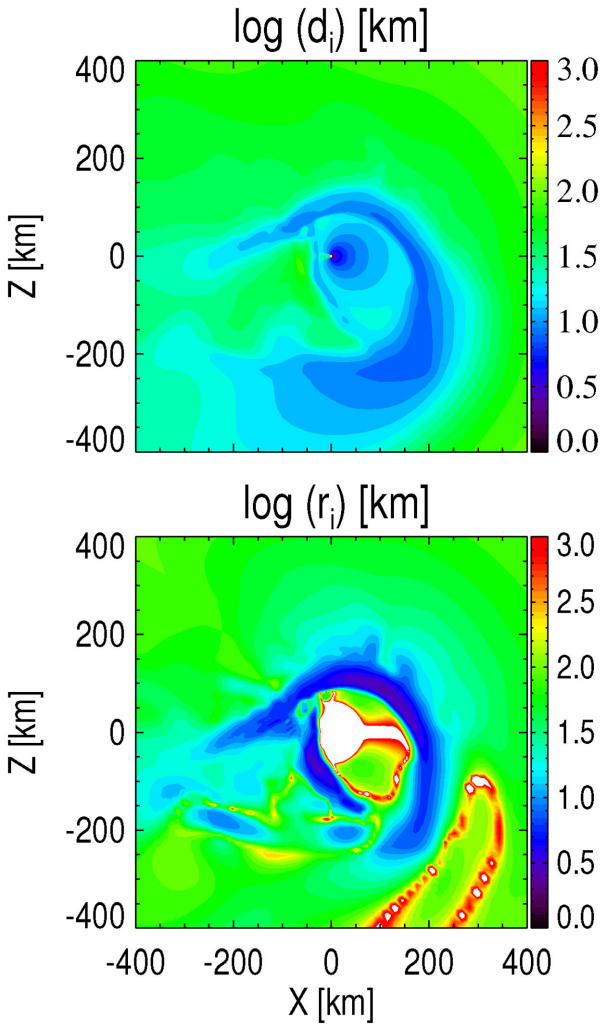

Figure 6. The ion inertial length and the ion gyro radius for the cometary ion within 400 km of the nucleus on the $y = 0$ plane.

ACKNOWLEDGEMENTS

This work was supported by the contracts Jet Propulsion Laboratory no. 1266313 and no. 1266314 from the US Rosetta Project and NASA grant NNX14AG84G from the Planetary Atmospheres Program.

The authors would like to thank the ROSINA team for supporting this research. The authors also thank the ESA Rosetta team for providing the opportunities to study this unique comet and their continuous support.

The authors would like to acknowledge the following high-performance computing resources: Yellowstone (ark:/85065/d7wd3xhc), provided by NCAR's Computational and Information Systems Laboratory, sponsored by the National Science Foundation; Pleiades, provided by the NASA Supercomputer Division at Ames; and Extreme Science and Engineering Discovery Environment (XSEDE), supported by National Science Foundation grant number ACI-1053575.

REFERENCES

Bagdonat T., Motschmann U., 2002, Earth Moon Planets, 90, 305
Birn J. et al., 2001, J. Geophys. Res., 106, 3715
Bougher S. et al., 2015, Science, 350, 0459
Cravens T. E., 1986, in Battrick B., Rolfe E. J., Reinhard R., eds, ESA SP-250: ESLAB Symposium on the Exploration of Halley's Comet. ESA, Noordwijk, p. 241
Deca J., Divin A., Henri P., Eriksson A., Markidis S., Olshevsky V., Horányi M., 2017, Phys. Rev. Lett., 118, 205101
Dorelli J. C., Glocer A., Collinson G., Tóth G., 2015, J. Geophys. Res., 120, 5377
Galeev A. A., Cravens T. E., Gombosi T. I., 1985, ApJ, 289, 807
Goetz C. et al., 2016a, MNRAS, 462, S459
Goetz C. et al., 2016b, A&A, 588, A24
Gombosi T. I., 2015, Physics of Cometary Magnetospheres. Wiley, New York, p. 169
Gombosi T. I., De Zeeuw D. L., Häberli R. M., Powell K. G., 1996, J. Geophys. Res., 101, 15233
Hansen K. C. et al., 2007, Space Sci. Rev., 128, 133
Huang Z. et al., 2016a, J. Geophys. Res.: Space Phys., 121, 4247
Huang Z. et al., 2016b, MNRAS, 462, S468
Koenders C., Glassmeier K.-H., Richter I., Motschmann U., Rubin M., 2013, Planet. Space Sci., 87, 85
Koenders C., Glassmeier K.-H., Richter I., Ranocha H., Motschmann U., 2015, Planet. Space Sci., 105, 101
Koenders C., Goetz C., Richter I., Motschmann U., Glassmeier K.-H., 2016, MNRAS, 462, S235
Ma Y. J. et al., 2011, J. Geophys. Res., 116, A10213
Madanian H. et al., 2017, AJ, 153, 30
Mandt K. E. et al., 2016, MNRAS, 462, S9
Müller J., Simon S., Motschmann U., Schüle J., Glassmeier K.-H., Pringle G. J., 2011, Comput. Phys. Commun., 182, 946
Najib D., Nagy A. F., Tóth G., Ma Y., 2011, J. Geophys. Res., 116, 5204
Neubauer F. M. et al., 1986, Nature, 321, 352
Powell K. G., Roe P. L., Linde T. J., Gombosi T. I., de Zeeuw D. L., 1999, J. Comput. Phys., 154, 284
Reme H. et al., 1986, Nature, 321, 349
Rubin M., Hansen K. C., Combi M. R., Daldorff L. K. S., Gombosi T. I., Tenishev V. M., 2012, J. Geophys. Res., 117, A06227
Rubin M. et al., 2014, icarus, 242, 38
Rubin M. et al., 2015, J. Geophys. Res., 120, 3503
Tóth G. et al., 2012, J. Comput. Phys., 231, 870
Wedlund C. S. et al., 2017, A&A, 604, A73

SUPPORTING INFORMATION

Supplementary data are available at *MNRAS* online.

reconnection_moive_view2.avi
reconnection_moive_view1.avi
inner_coma_movie.mp4

Please note: Oxford University Press is not responsible for the content or functionality of any supporting materials supplied by the authors. Any queries (other than missing material) should be directed to the corresponding author for the article.

This paper has been typeset from a TEX/LATEX file prepared by the author.